IOP Conference Series:
Materials Science and
Engineering

PAPER • **OPEN ACCESS**

Ethylene Gas Sensing Properties of Tin Oxide Nanowires Synthesized via CVD Method

To cite this article: Maisara A. M. Akhir *et al* 2018 *IOP Conf. Ser.: Mater. Sci. Eng.* **318** 012038

IOP Conf. Series: Materials Science and Engineering **318** (2018) 012038 doi:10.1088/1757-899X/318/1/012038

Ethylene Gas Sensing Properties of Tin Oxide Nanowires Synthesized via CVD Method

Maisara A. M. Akhir[1*], Khairudin Mohamed[2], Sheikh A. Rezan[3], M. M. Arafat[4], A. S. M. A. Haseeb[4], M. N. A. Uda[1] and Nuradibah, M. A.[1]
[1]School of Bioprocess Engineering, Universiti Malaysia Perlis, 02600 Arau, Perlis, Malaysia
[2]School of Mechanical Engineering, Universiti Sains Malaysia, 14300 Nibong Tebal, Penang, Malaysia
[3]School of Materials & Mineral Resources Engineering, Universiti Sains Malaysia, 14300 Nibong Tebal Penang, Malaysia
[4]Department of Mechanical Engineering, Faculty of Engineering, University of Malaya, 50603 Kuala Lumpur, Malaysia

E-mail: maisaraazad@unimap.edu.my

Abstract. This paper studies ethylene gas sensing performance of tin oxide (SnO_2) nanowires (NWs) as sensing material synthesized using chemical vapor deposition (CVD) technique. The effect of NWs diameter on ethylene gas sensing characteristics were investigated. SnO_2 NWs with diameter of ~40 and ~240 nm were deposited onto the alumina substrate with printed gold electrodes and tested for sensing characteristic toward ethylene gas. From the finding, the smallest diameter of NWs (42 nm) exhibit fast response and recovery time and higher sensitivity compared to largest diameter of NWs (~240 nm). Both sensor show good reversibility features for ethylene gas sensor.

1. Introduction

Ethylene, C_2H_4 gas is a vegetal hormone and produced in most plant tissues and is known to be an influential factor in starting off the ripening of fruits. Furthermore, ethylene gas is an important substance in fresh argo-products marketing because it can be used commercially for artificial plant hormone and to monitor the ripening process of climacteric fruits. This has made it possible for tropical fruits such as mangoes and bananas to be harvested green and shipped to distant markets, where they are ripened under controlled conditions. However, natural ethylene production of fruits can cause problems in storage facilities. Ethylene can destroy the green color of plants.

Realizing the importance of detecting the ethylene gas, many researchers are focusing on the investigation of the most suitable sensing material for the ethylene gas sensor. Various sensing materials had been used to detect low concentration of ethylene including titanium dioxide (TiO_2) thin films [1], porous indium oxide (In_3O_3) nanospheres [2], tungsten trioxide (WO_3) thick film [3] and SnO_2 nanoparticles [4, 5]. Most of the materials mentioned above are used to model chemiresistive-based devices, where the conductivity of these materials either increases or decreases based on the exposure to different gas concentrations.

Among these materials, SnO_2 nanoparticles are the most popular material for ethylene gas sensor due to its wide band gap n-type semiconductor properties, which leads to low electrical resistance and better electrical conductivity for gas sensing properties. Furthermore, low operating temperature, high

sensitivity, mechanical simplicity of sensor design and low manufacturing cost have made SnO_2 the preferred choice for gas sensor applications.

Besides, SnO_2 nanostructures has the ability to change its electrical and micro structural properties depending on its size and shape [6]. For example, one dimensional (1-D) nanostructured SnO_2 in the form of wires, tubes, belts with high aspect ratio offer unique surface properties. This includes photoluminescence and gas sensitive resistivity with better crystallinity, higher density, and lower power consumption [7, 8]. Properties of the materials such as melting point, electrical conductivity, chemical reactivity, fluorescence and magnetic permeability are size-dependent in the nano-scale range and these properties change as a function of the size of the particles. Recently, 1-D nanostructures have attracted much attention because of their potential applications in gas sensors due to its high surface to volume ratio, while maintaining good chemical and thermal stabilities with minimal power consumption and low weight.

In our previous paper, detail discussion on CVD synthesis and characterization method had been discussed [9]. In this paper, gas sensing performance of 1-D SnO_2 nanostructures toward ethylene gas were investigated in terms of sensitivity, response and recovery times, optimum operating temperature and reversibility features. SnO_2 NWs were synthesized using CVD technique.

2. Materials and Methods

2.1. Synthesis and Characterization

The details for the synthesis and characterization of SnO_2 NWs are described in our previous work [9]. The sample with the largest, C8 (~250 nm) and smallest, C7 (42 nm) diameter of NWs were selected for gas sensing properties test. Figure 1 shows the SEM images and X-ray diffraction spectroscopy (XRD) for the studied samples. XRD results confirm the formation of the tetragonal rutile structure of SnO_2 (ICSD # 98-005-8477).

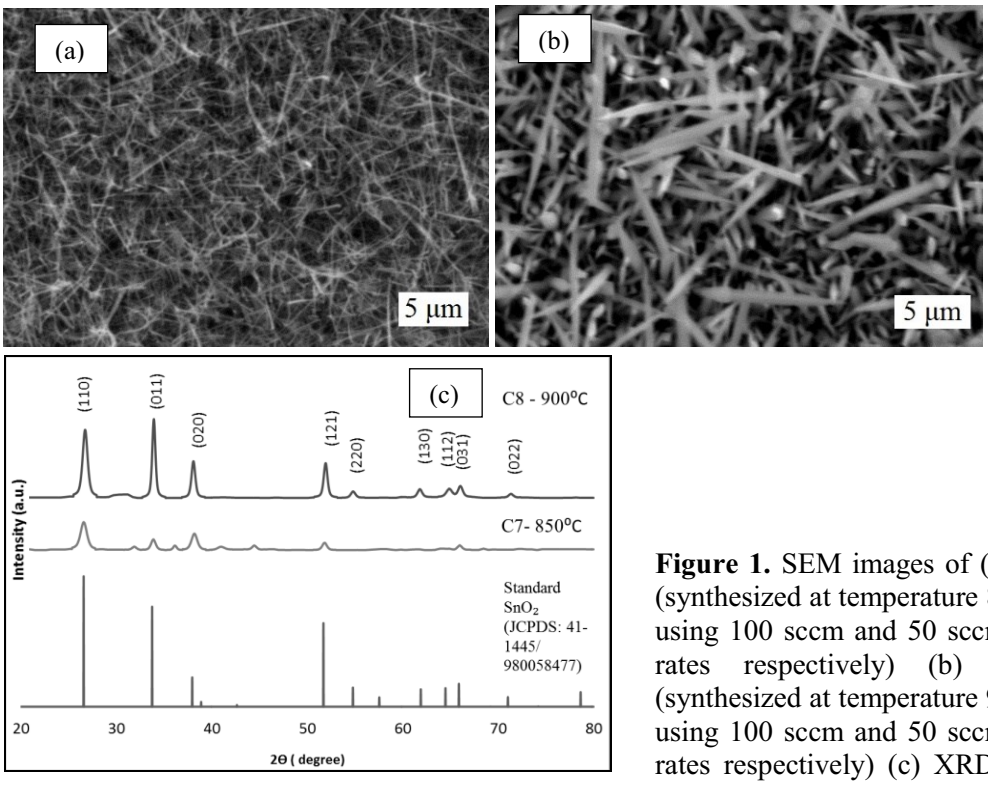

Figure 1. SEM images of (a) smallest NWs, C7 (synthesized at temperature 850°C for 60 minutes using 100 sccm and 50 sccm of Ar and O_2 flow rates respectively) (b) largest NWs, C8 (synthesized at temperature 900°C for 60 minutes using 100 sccm and 50 sccm of Ar and O_2 flow rates respectively) (c) XRD spectra for C7 and C8.

2.2. Gas sensing performance test

The as-prepared SnO_2 NWs were mixed with sensor ink [10] and drop coated onto the alumina substrate with interdigitated printed Au electrodes on the top of its surfaces for gas sensing element fabrication. The sensing element was sintered in a furnace at temperature of 500 °C for 1 hour under nitrogen flow rate of 200 sccm at which the phase contents were stabilized.

In studying the gas sensing performances of SnO_2 nanostructures, several parameters had been selected, which were sensitivity, optimum operating temperature, response time and recovery time. Response time is the time gap needed by the sensing material to reach 90 % of its steady-state resistance value after the introduction of ethylene gas. On the other hand, the recovery time is the time gap of gas sensing material to be within 10 % of its resistance value before exposure to the ethylene gas. These two responses were obtained by measuring the time interval of resistance versus time graph. The sensitivity of the sensor is defined as Ra/Rg, where Ra and Rg is the resistance of the sensor in air and in the target gas, respectively. The sensing materials had been tested under different working temperatures. The temperature with the highest sensitivity value will be considered as the optimum operating temperature and was used to measure the gas response at different ethylene concentrations.

The electrodes of gas sensing element were then connected to the electrometer by using gold wires and the electrometer was connected to a PC. Then, the elements were placed inside the quartz tube and inserted in the furnace. N_2 air was allowed to flow inside the test chamber at the pre-set temperature until the stable resistance was obtained. After that, an ethylene gas pulse was discharged for a certain period of time, followed by the nitrogen gas pulse and the process was repeated for different working temperature. The change in resistance in the nitrogen gas and ethylene gas over time was recorded. The dilution of target gas concentrations ranging from 50 to 100 ppm was done using digital mass flow controller (C100L-CM-NR-2-0V1-SV1-PV2-V1, Sierra) and the total flow rate of gases was maintained at 500 sccm throughout the experiments. Figure 2 illustrates the schematic diagram of gas sensing measurement system.

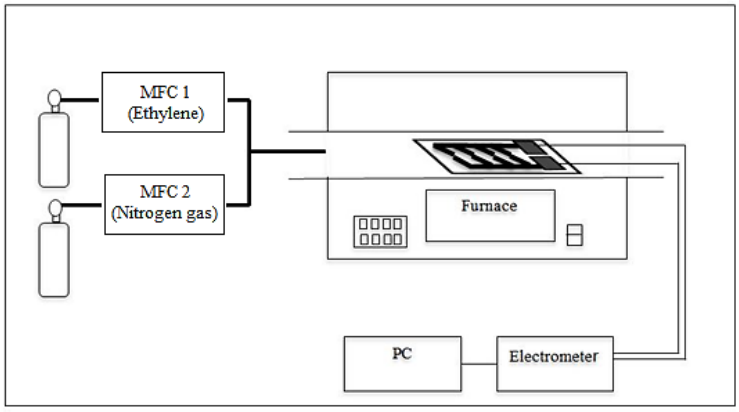

Figure 2. The schematic diagram of the gas sensing measurement system. This system was connected to a computer via the specific interface board. Data were collected in the form of resistance and temperature in real-time.

3. Results and Discussions

Figure 3 illustrates graph sensitivity versus temperature for both of the CVD samples. From the figure 3, the sensitivities of SnO_2 NWs with the smallest (C7) and the largest diameter (C8) to ethylene gas had increased when the temperature was increased. Furthermore, both sensors reached the maximum values when the temperature was at 450°C. Besides this, it can be seen that the sensor with the smallest diameter (C7) NWs had higher sensitivity of 10.55 than the sensor with the largest diameter by a magnitude of 6.54. The sensitivity difference between the smallest and largest diameter NW was about 38 %.

Table 1 presents the response and recovery times of SnO_2 NWs after exposure to 1000 ppm concentration of ethylene gas at different temperatures. The response time of the sensor with the largest diameter (C8) was much longer than the sensor with the smallest diameter (C7) at temperature 375 °C. On the other hand, between temperature 400 °C – 450 °C for CVD sample C8, the response time was similar to C7 which was less than 10 s. It should be noted that the scan time of the resistance measurement in this system was every 10 s. So, the sensors probably took less than 10 s to response to the changes in resistivity.

Besides this, the smallest diameter of SnO_2 NWs took less than 1 minute to recover to 90 % of the baseline resistance in comparison to the largest NWs, which took more than 1 minute to recover. The recovery times for both samples increased with operating temperature. From the results, it can be concluded that the sensor with the smallest diameter of NWs (C7) had better response and recovery times compared to the sensor with the largest diameter (C8).

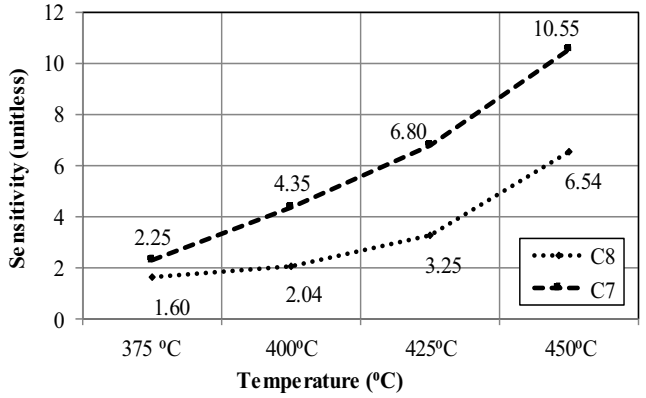

Figure 3. Sensitivity change with respect to temperature for CVD samples C7 and C8.

Table 1. Response and recovery time of SnO_2 NWs towards 1000 ppm concentration of ethylene.

Temperature (°C)	Response Time (s)				Recovery Time (s)			
	375	400	425	450	375	400	425	450
C7	≤10	≤10	≤10	≤10	20	30	50	50
C8	20	≤10	≤10	≤10	60	70	80	90

* ≤ 10 meant the response time may be equal to or less than 10s since the system measured resistance values every 10s.

The sensor's response characteristics toward various ethylene gas concentrations at the optimum temperature of 450 °C were investigated. This operating temperature of 450 °C was chosen based on sensitivity results in figure 3. Figure 4 (a)-(c) shows the sensor response characteristic at various ethylene gas concentrations. From the figure, it can be observed that the resistance of both sensors decreases steeply upon the exposure to ethylene gas and gradually increases after a specific recovery time. Moreover, based on figure 4 (c), the magnitude of the gas sensitivities for both of the sensors improved dramatically with the increase in ethylene gas concentrations. SnO_2 NWs with the smallest diameter (C7) had a higher gas sensitivity value response at all concentration compared to the largest diameter of NWs's (C8) sensor.

In terms of reversibility, both sensors showed excellent ability to recover to its initial value after exposure to the analyte gas was removed. As seen in figure 4 (a) and (b), the resistances in sample C7

and C8 had reached their baseline value upon removal of ethylene gas. It was noticeable that the baseline resistance for C7 was higher than C8 by ~96.8 % at 1000 ppm of ethylene. This difference may be due to the smaller NWs diameter sample having a larger electron depleted region. As a result of this, a higher resistance was obtained with the smaller diameter NWs. Similar observation was reported by Yamazaki [11] and the explanation for this was centered on the depleted region.

Furthermore, a shorter response and recovery time of the SnO_2 NWs was found at high ethylene gas concentration (1000 ppm) and this response and recovery time had increased with decreasing gas concentration. The response and recovery time for C7 were between 10 s – 20 s (1000 ppm) and 50 s - 80 at lower concentration (50 ppm). For sample C8, it was 10 s – 20 s at high concentration and 1 minutes - 2 minutes at lower concentration.

1D nanostructures offer an advantage in terms of high aspect ratio (L/D) ratio, which allows a larger active site surface for gas adsorption and desorption in gas sensor applications. Typical range for aspect ratio was between 5 – 1000 [12]. The high aspect ratio for SnO_2 NWs was expected to provide high gas sensitivity. Based on the findings in the present work, the surface reaction of the SnO_2 NWs gas sensor greatly depended on the working temperature. It was noticed that the resistance of SnO_2 NWs decreases with increase of temperature and followed closely to Ohm's law. During the increase in operating temperature while gas sensing, the adsorption and desorption processes of the gas molecules will be accelerated. The captured electrons by the adsorbed oxygen atom in SnO_2 are thermally excited to the conduction band as the temperature rises. Hence, this results in a decrease in resistivity.

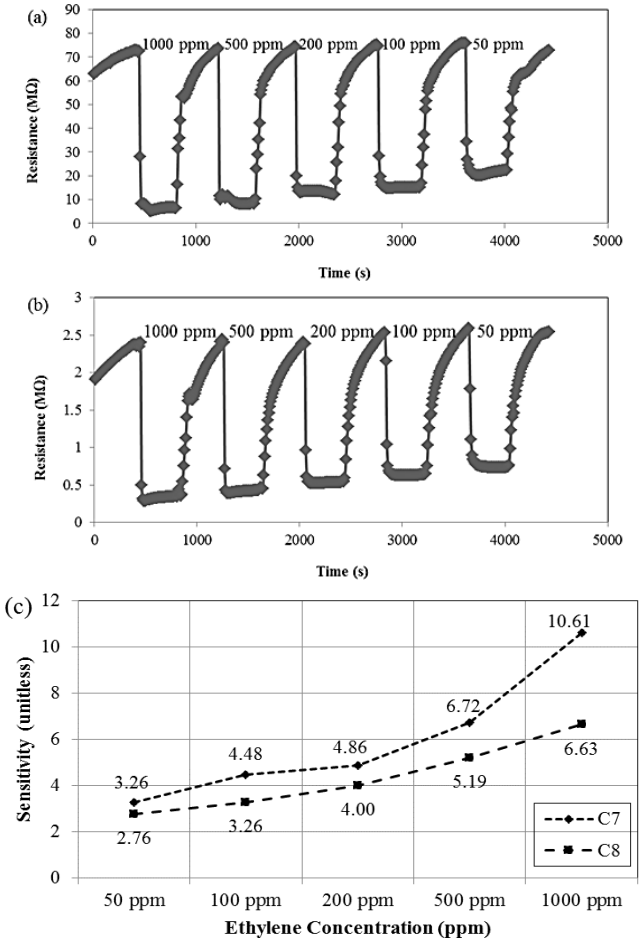

Figure 4. Gas sensitivity response with respect to ethylene gas (a) C7, (b) C8 and (c) varying ethylene gas concentration at temperature of 450°C.

Furthermore, at low temperature (<150 °C), the adsorbed oxygen species at the surface of sensing material will extract the electrons from the conduction band of the material to produce O_2^- by equation (2) [13]. At the same time, O^- and O^{2-} are produced when the temperature was between 150 °C to 450 °C (Equation 3 and 4) and O^- becomes dominant at this temperature [13,14]. In the latter case, the highest sensitivity of 10.61 was measured for SnO_2 NWs via CVD at 450 °C. Therefore, O^- atoms absorbed onto the NWs surface was believed to be the predominant oxygen species at this temperature based on studies by Ahsan [13].

The expected reactions between the analyte gas and oxide surface of the sensing material at elevated temperatures are written in equation (3) and (5). The sensing mechanism of SnO_2 material towards ethylene gas involves the adsorption of oxygen molecules from the atmosphere onto the SnO_2 surface. In the present study gas sensing setup, the origin of the oxygen molecule was from the premixed ethylene and air gas mixture. This chemisorbed oxygen species was formed by trapping of electrons from the conduction band of SnO_2. As a result of this trapping, a depletion layer consists of O^- ionic species was formed. This process is expressed in equation (3).

The depletion region size increases and the conduction band decreases as more and more oxygen molecules are adsorbed onto the sensing surface. This in turn causes a low electrical conductivity or high surface resistivity on the SnO_2 NWs. When the ethylene gas is exposed to SnO_2 sensing layer at an elevated temperature, the molecules will react with the adsorbed species and this process will revert back the electrons to the SnO_2 conduction band as given in equation (5). The high electron concentrations result in higher surface conductivity and thus, the resistance will decrease [5]. The decrease in resistivity will signal the presence of ethylene gas. Figure 5 illustrates the schematic diagram of the depletion and conduction region before and after exposure to ethylene gas.

$$O_2\,(g) \rightarrow O_2\,(ads) \quad (1)$$
$$e^- + O_2\,(ads) \rightarrow O_2^-\,(ads) \quad (2)$$
$$2e^- + O_2\,(ads) \rightarrow 2O^-\,(ads) \quad (3)$$
$$e^- + O^-\,(ads) \rightarrow O^{2-}\,(ads) \quad (4)$$
$$C_2H_4 + O^{2-} \rightarrow C_2H_4O + 2e^- \quad (5)$$

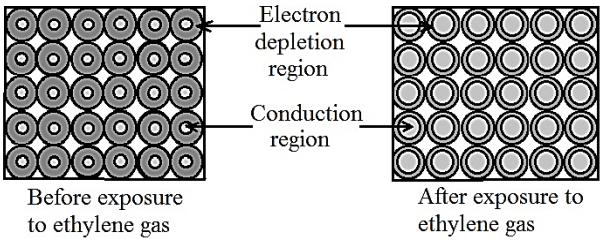

Figure 5. The schematic diagram of the depletion and the conduction region before and after exposure to ethylene gas.

With reference to the table 1 and figure 4, both SnO_2 NWs exhibit fast response and recovery time, which was 10 s to 20 s (C7) and 50 s to 120 s (C8) respectively upon exposure to ethylene gas. This response and recovery behavior was due to the high surface area of SnO_2 NWs structure that were randomly oriented. This randomization allows rapid diffusion between the NWs gaps or voids with a shorter time required to return to baseline resistance. Furthermore, gas sensitivity behavior for C7 and C8 show that it has the ability to recover to its initial baseline resistance when ethylene gas was purged with nitrogen from the test chamber. These findings implied a good reversibility property of the sensor with NWs like structure synthesized using CVD methods.

Besides this, SnO_2 NWs with the smallest diameter (C7) had higher sensitivity values than the largest diameter NWs (C8) at all relative ethylene gas concentrations at 450 °C. Wire-like structure of C7 and C8 allowed the gas molecules to absorbed on the NWs with ease. Figure 6 presents the illustration of the potential difference between the intra-particles connection of SnO_2 NWs.

From the figure, it can be seen that the geometrical aspect (L/D) of the NWs affects the resistance of the sensor by changes in the conduction (E_C) and Fermi energy levels (E_F). These changes are mostly governed by the bulk interface and interface between the electrode and sensing NWs rather than the grain boundaries [11].

The higher gas sensitivity of the smallest NW diameter (C7) compared to largest (C8) was due to a wider conductive bulk region in the smaller diameter sample (refer to figure 6). The smaller NWs have more inter-grain contacts and in turn enhances the gas sensitivity than the larger NWs. Therefore, the conductance of the bulk region for the NWs was influenced by its exposure to ethylene gas. This exposure led to a large change in surface resistivity and higher gas sensitivity for sample C7 than C8.

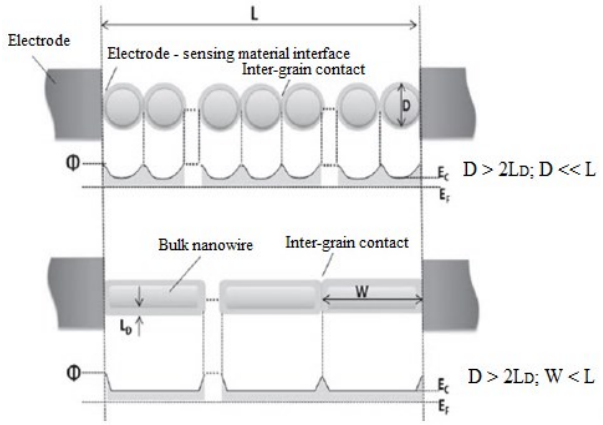

Figure 6. The illustration of the potential intra-particles connection SnO_2 NWs [11]

4. Conclusions

CVD sample with the smallest NWs diameter (C7) exhibit the quickest response and recovery time towards ethylene gas than the largest NWs diameter (C8) samples. Moreover, the gas sensitivity was higher for smallest diameter of NWs than the largest diameter. In addition, the 1-D NWs shows a good reversibility characteristic with the lowest recovery time among the tested samples (50 s). This work shows successful fabrication of 1-D SnO_2 NWs gas sensing material to detect low concentrations of ethylene gas.

Acknowledgments

The author is grateful to School of Bioprocess Engineering, UniMAP, Nanofabrication and Functional Materials Lab, School of Mechanical Engineering, USM and Department of Mechanical Engineering, Faculty of Engineering, UM, for providing the facilities to carry out the research. The research is funded by UniMAP/STG/2016/9001-00553.

References

[1] R. Zhang, M. I. Tejedor, M. A. Anderson, M. Paulose, and C. A. Grimes, "Ethylene Detection Using Nanoporous $PtTiO_2$ Coatings Applied to Magnetoelastic Thick Films," *Sensors*, **2002**, 331 (2002).

[2] Y. Cao *et al.*, "Synthesis of porous In_2O_3 microspheres as a sensitive material for early warning of hydrocarbon explosions," *RSC Adv.*, **5**, 5424 (2015).

[3] O. Nimittrakoolchai and S. Supothina, "High-yield precipitation synthesis of tungsten oxide platelet particle and its ethylene gas-sensing characteristic," *Mater. Chem. Phys.*, **112**, 270 (2008).

[4] W. Chen, Q. Zhou, T. Gao, X. Su, and F. Wan, "Pd-Doped SnO_2-Based Sensor Detecting Characteristic Fault Hydrocarbon Gases in Transformer Oil," *J. Nanomater.*, **2013**, 1 (2013).

[5] M. Agarwal, M. D. Balachandran, S. Shrestha, and K. Varahramyan, "SnO_2 Nanoparticle-Based Passive Capacitive Sensor for Ethylene Detection," *J. Nanomater.*, **2012**, 1 (2012).
[6] C. H. Drake, "Understanding the Low Temperature Electrical Properties," (2007).
[7] Y. H. Y. and G. W. Y. B Wang, "Growth mechanisms of SnO_2/Sn nanocables," *Nanotechnology*, **17**, 7 (2006).
[8] H.-C. Z. Hang Chi Hong-Jun Xu, Xu-Dong Shan, Zhi-Min Liao, and Da-Peng Yu, "One-Step Growth and Field Emission Properties of SnO_2-Capped Silicon Nanowires: A Sn-Catalyzed Approach," *J. Phys. Chem.*, **113**, 4 (2009).
[9] M. A. M. Akhir, K. Mohamed, S. A. Rezan, H. L. Lee, and S. S. M. Izah, "An assessment of chemical vapor deposition synthesis of SnO_2 nanowires by statistical design," *Key Engineering Materials*, **701**, 52 (2016).
[10] M. Arafat, A. Haseeb, and S. Akbar, "A Selective Ultrahigh Responding High Temperature Ethanol Sensor Using TiO_2 Nanoparticles," *Sensors*, **14**, 13613 (2014).
[11] T. Yamazaki, "Formation of oxide nanowires by thermal evaporation and their application to gas sensors," *Nanowires - Implementations Appl.*, **7**, 117 (2012).
[12] J. Huang and Q. Wan, "Gas sensors based on semiconducting metal oxide one-dimensional nanostructures," *Sensors*, **9**, 9903 (2009).
[13] M. Ahsan, "Thermally Evaporated Tungsten Oxide (WO_3) Thin Films for Gas Sensing Applications," (2012).
[14] C. Wang, L. Yin, L. Zhang, D. Xiang, and R. Gao, "Metal oxide gas sensors: sensitivity and influencing factors.," *Sensors (Basel).*, **10**, 2088 (2010).